A Molecular Orbital Analysis of the Regioselectivity of Nucleophilic Addition to η^3-Allyl Complexes and the Conformation of the η^3-Allyl Ligand in $L_3(CO)_2(\eta^3\text{-}C_3H_5)Mo^{II}$ Complexes

M. David Curtis* and Odile Eisenstein

Department of Chemistry, The University of Michigan, Ann Arbor, Michigan 48109

Received November 14, 1983

Extended Hückel (EHMO) calculations have been employed to elucidate the electronic factors responsible for the rotational preference observed for the allyl group in $X_3(CO)_2(\eta^3\text{-allyl})Mo^{II}$ complexes and to determine the factors responsible for the observed regioselectivity of nucleophilic addition to a variety of η^3-allyl complexes. The rotational preference of the allyl group is traced to a hybridization of the metal orbitals due to the strongly π-bonding carbonyl ligands. The preference for nucleophiles to attack the terminal carbon of the η^3-allyl moiety is shown to be due to frontier obtital control as opposed to charge control. The electronic requirements for nucleophilic addition to the central carbon of the η^3-allyl are presented.

Introduction

η^3-Allyl complexes have proved to be valuable intermediates for the formation of new C–C bonds by way of nucleophilic attack on the coordinated allyl group.[1] With one exception, nucleophiles attack the η^3-allyl group at one of the terminal carbons to give olefins (eq 1).[1] The sole

(1)

reported exception to the regioselectivity shown in eq 1 is the nucleophilic attack by H^- or R^- on the $Cp_2M(\eta^3\text{-allyl})$ cations (M = Mo, W) to give metallocyclobutanes 1 (eq 2).[2]

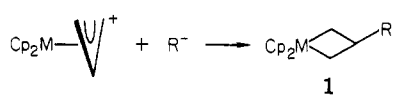

(2)

1

Several years ago, the reactions of cationic, 16-electron η^3-allyl complexes with nucleophiles were being investigated in our laboratories with the object of preparing reactive metallocyclobutanes and studying the latter in connection with the olefin methathesis reaction.[3] One of the complexes that was prepared and structurally characterized was the chloride-bridged dimer $[(bpy)(CO)_2(\eta^3\text{-}C_3H_5)Mo]_2(\mu\text{-}Cl)BF_4$.[4] On each Mo atom, the coordinated η^3-allyl group adopted a conformation that placed the open face of the allyl group toward the adjacent cis $(CO)_2$ grouping.

In fact, *all* d^4 $L_2XMo(\eta^3\text{-}C_3H_5)(CO)_2$ complexes whose structures have been determined display the orientation of the η^3-allyl group as shown in **2** or **3**. With L_2X = (CH_3CN),[5c] (bpy)(SCN),[6a] (phen)(SCN),[6a] $PhB(pz)_3$,[7b] $Et_2B(pz)_2(py)$,[7c] Cl_3,[5c] $H_2B(3,5\text{-}Me_2pz)$,[7d] (bpy)(py),[6b] (bpy)Cl, or $(MeOCH_2CH_2OMe)(CF_3CO_2)$[6c] the structure adopted by $L_2XMo(\eta^3\text{-}C_3H_5)(CO)_2$ is **2**. When L_2X is (diphos)(Cl), structure **3** is adopted in the solid state, but the diphos complexes are fluxional in solution.[8] The Cp group is a special case of L_2X, and $CpMo(CO)_2(\eta^3\text{-}C_3H_5)$ also adopts structure **2** in the solid.[7e] Several complexes in which the allyl residue is part of a larger ring also exhibit structure **2**.[7b,f]

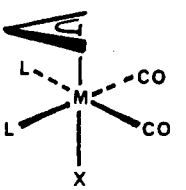

(2)

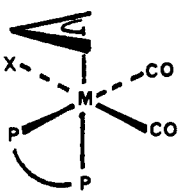

(3)

Since the orientation of the η^3-allyl residue always places its open face toward the two carbonyls, an electronic stabilization for this particular orientation is indicated. We have probed this stabilizing effect with the fragment molecular orbital (FMO) approach using the extended Hückel formalism (EHMO).[9] These calculations have also provided a rationale for the regioselectivity observed for nucleophilic attack on coordinated η^3-allyl groups. In par-

(1) (a) Henry, P. M. *Adv. Organomet. Chem.* **1975**, *13*, 363. (b) Trost, B. M. *Acc. Chem. Res.* **1980**, *13*, 385. (c) Bosnich, B.; Mackenzie, P. B. *Pure Appl. Chem.* **1982**, *54*, 189. (d) Tsuji, J. *Ibid.* **1982**, *54*, 197. (e) Pauson, P. L. *J. Organomet. Chem.* **1980**, *200*, 207.

(2) Ephretikhine, M.; Francis, B. R.; Green, M. L. H.; Mackenzie, R. E.; Smith, M. J. *J. Chem. Soc., Dalton Trans.* **1977**, 1131.

(3) (a) Puddephatt, R. J. *Coord. Chem. Rev.* **1980**, *33*, 149. (b) Katz, T. J. *Adv. Organomet. Chem.* **1977**, *16*, 283. (c) Grubbs, R. H. *Prog. Inorg. Chem.* **1978**, *24*, 1.

(4) Curtis, M. D.; Fotinos, N. A. *J. Organomet. Chem.*, in press.

(5) (a) Drew, M. G. B.; Brisdon, B. J.; Edwards, D. A.; Paddick, K. E. *Inorg. Chim. Acta* **1979**, *35*, 1381. (b) Prout, K.; Rees, G. V. *Acta Crystallogr., Sect. B* **1974**, *B30*, 2251. (c) Drew, M. G. B.; Brisdon, B. J.; Cartwright, M. *Inorg. Chim. Acta* **1979**, *36*, 127.

(6) (a) Graham, A. J.; Fenn, R. H. *J. Organomet. Chem.* **1969**, *17*, 405; **1970**, *24*, 173. (b) Fenn, R. H.; Graham, A. J. *Ibid.* **1972**, *37*, 137.

(7) (a) Graham, A. J.; Akrigg, D.; Sheldrick, B. *Cryst. Struct. Commun.* **1976**, *5*, 891. (b) Cotton, F. A.; Murillo, C. A.; Stults, B. R. *Inorg. Chim. Acta* **1977**, *22*, 75. (c) Cotton, F. A.; Frenz, B. A.; Stanislowski, A. G. *Ibid.* **1973**, *7*, 503. (d) Kosky, C. A.; Ganis, P.; Avatabile, G. *Acta Crystallogr., Sect. B* **1971**, *B27*, 1859. (e) Faller, J. W.; Chodosh, D. F.; Katahira, D. *J. Organomet. Chem.* **1980**, *187*, 227. (f) Cotton, F. A.; Jeremic, M.; Shaver, A. *Inorg. Chim. Acta* **1972**, *6*, 543.

(8) Faller, J. W.; Haitko, D. A.; Adams, R. D.; Chodosh, D. F. *J. Am. Chem. Soc.* **1979**, *101*, 865.

(9) The calculations were performed by using R. Hoffmann's programs ICON8 and FMO with the weighted H_{ij} option: Ammeter, J. H.; Burgi, H.-B.; Thibeault, J. C.; Hoffmann, R. *J. Am. Chem. Soc.* **1978**, *100*, 3686. The atomic parameters are described in: Kubacek, P.; Hoffmann, R.; Halvas, Z. *Organometallics* **1982**, *1*, 180. Hoffman, D. M.; Hoffman, R. *J. Am. Chem. Soc.* **1982**, *104*, 4858. Hoffmann, R., private communication (Pd parameters).

0276-7333/84/2303-0887$01.50/0

ticular, we show that frontier orbital control, rather than charge control, directs attacking nucleophiles to the terminal carbon atoms of the η^3-allyl group (eq 1). Only under certain special conditions will the frontier orbital allow attack at the central carbon (eq 2).

Discussion

Conformational Preference of the Allyl Group in $X_3(CO)_2(\eta^3\text{-}C_3H_5)Mo^{II}$ Complexes. Before describing the EHMO results, it is instructive to first analyze the conformation problem in terms of the isolobal relationships developed by Hoffmann and co-workers.[10] The d^4 ML_5 fragment is isolabal with CH^+. Therefore, the $L_5M(\eta^3\text{-}C_3H_5)$ group is isolobal with $(CH^+)(C_3H_5^-)$ or bicyclobutane:

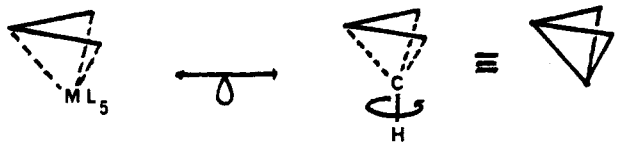

There should be no barrier to rotation of the C_3H_5 fragment about the isolobal C–H group. Hence we expect (and find) only a relatively small, second-order effect to be responsible for the rotational preference of the η^3-C_3H_5 group in the $L_2XMo(\eta^3\text{-}C_3H_5)(CO)_2$ complexes.

FMO analyses were made on the model compounds $(HCN)_3(CO)_2Mo(\eta^3\text{-}C_3H_5)^+$ and $Cl_3(CO)_2Mo(\eta^3\text{-}C_3H_5)^-$ (see Appendix for details). The former models the $L_2X(CO)_2Mo(\eta^3\text{-}C_3H_5)$ complexes with weakly π-accepting ligands and the latter π-donor L_2X ligands. Calculations were performed for three orientations (θ = 0.0°, 90.0°, and 180°) of the allyl group as defined below. No attempt was made to optimize the geometry of the rotamers. The total energies of the three rotamers (referenced to E (θ = 0.0°) = 0.0) are also shown.

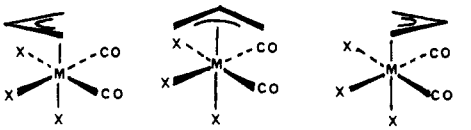

X	θ = 0.0°	90°	180°
ΔE: HCN	0.0	6.1	14.7 kcal/mol
ΔE: Cl	0.0	7.6	10.1

The EHMO method correctly calculates the θ = 0.0° rotamer to have the lowest energy by 10–15 kcal/mol, a reasonable value for the rotation barrier in complexes of this type. Furthermore, a rotation–energy profile with only one minimum, as found here, precludes the possibility of observing the rotation of the η^3-allyl by variable temperature NMR. Indeed, no evidence for allyl group rotation was seen in the variable temperature NMR studies of **3** which undergoes a trigonal twist of the P_2X-substituted face of the octahedron against the $(CO)_2(C_3H_5)$-substituted face.[8]

Since θ = 0.0° is the lowest energy conformation and θ = 180° the highest, the ensuing discussion will focus only on these two rotamers. The fragment orbitals of interest are the occupied π, n, and empty π^* orbitals of the allyl group and the frontier orbitals of the ML_5-type fragment. The frontier orbitals of the $X_3Mo(CO)_2$ fragment consist of the δ-type xy, two nearly degenerate π-type hybrids ($h_1 = xz - yz$ and $h_2 \simeq xz + yz$), and the σ-type hybrid composed mainly of z^2 at somewhat higher energies (Figure 1). The xy orbital interacts only weakly with the allyl

(10) Hoffmann, R. *Angew. Chem., Int. Ed. Engl.* **1982**, *21*, 711.

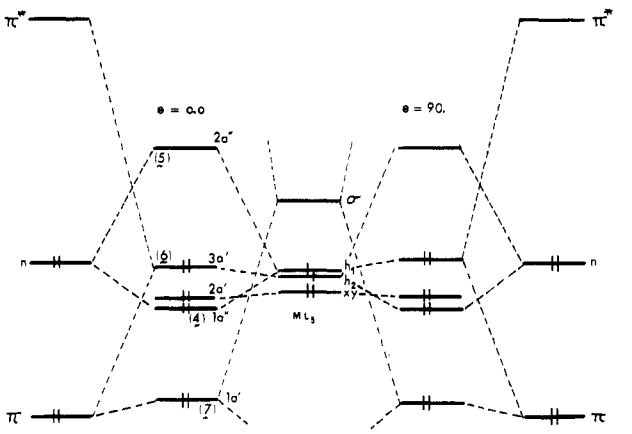

Figure 1. EHMO energy level diagram for the interaction of the d^4 $X_3(CO)_2Mo$ fragment with allyl fragment oribtals for two rotations of the allyl group. See text for a description of the orientation and orbitals.

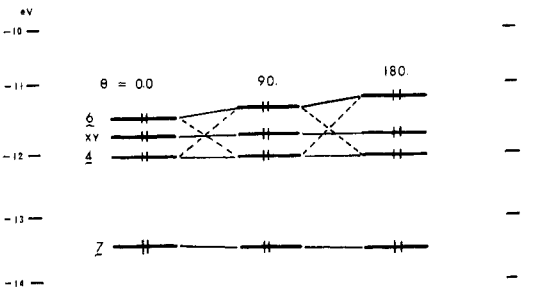

Figure 2. Variation of the energies of the filled MO's of $X_3(CO)_2Mo(\eta^3\text{-allyl})$ upon rotation of the allyl group. The dashed lines show the intended crossings.

FMO's and can be ignored. The antisymmetric nonbonding orbital (n) finds its symmetry match in the h_1 hybrid and forms bonding (**4**) and antibonding (**5**) combinations.

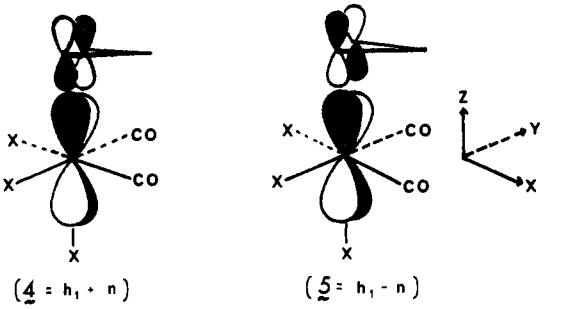

(**4** = h_1 + n) (**5** = h_1 − n)

The θ = 180° orientation for the allyl group is shown in **4** and **5**. This interaction is essentially equivalent in the θ = 0.0° orientation, and the filled bonding orbital **4** does not contribute to the rotation barrier (at θ = 90°, the bonding role of h_1 is taken over by h_2 and by linear combinations of $h_1 + h_2$ at intermediate angles (see Figures 1 and 2)).

The symmetric π and π^* orbitals both interact with the symmetric σ and h_2 ($xz + yz$) FMO's to form the bonding MO's shown in **6–8**. The energy of **8** is about 6 kcal/mol higher than that of **6**, so that the destabilization of the HOMO upon rotation of the allyl group accounts for nearly half of the total destabilization caused by the rotation of the allyl group from θ = 0.0° to θ = 180°. What is the source of this destabilization, and why is the contribution of the central carbon (C_2) to the MO's so different in the two rotamers?

The *group* overlap integrals of the π and π^* orbitals of

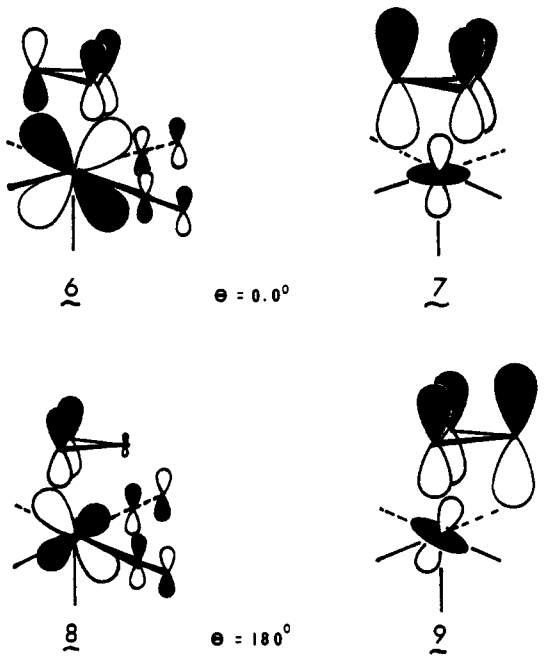

the allyl fragment with the h_2 hybrid are shown:

	$\theta = 0.0°$	$\theta = 180°$
$\langle\pi\|h_2\rangle$	0.010	0.133
$\langle\pi^*\|h_2\rangle$	0.097	0.087

The largest single difference is the much higher overlap of π with h_2 in the $\theta = 180°$ rotamer. Since π, being lower in energy than h_2, will mix into the final MO (6 or 8) in an antibonding manner, 8 will be destabilized more than 6 due to the larger overlap of h_2 with π in the 180° rotamer.

The quite different relative values of the C $2p_z$ coefficients associated with the allyl fragment in 6 and 8 are also a result of the mixing of the π and π^* FMO's in the final MO. In 6, the π and π^* mix so as to reinforce the bonding of the central carbon (C_2) to the metal. Conversely, in 8 the π and π^* mix is such a way that a virtual node is created at C_2.

To understand this behavior, we must take a closer look at the $X_3(CO)_2Mo$ fragment orbitals. The σ orbital is not pure z^2 but is hybridized with 5s, $5p_z$, and $(xz + yz)$: $\sigma = 0.18\ (5s) + 0.34\ (5p) + 0.6\ (z^2) - 0.22\ (xz + yz) + \ldots$ (eq 3). The admixture of $(xz + yz)$ tilts the σ orbital toward

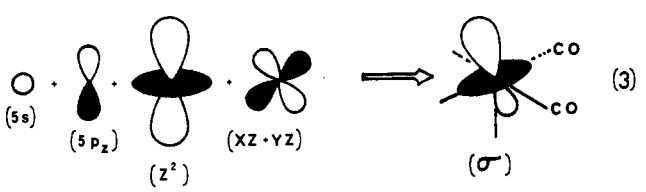

(3)

the C_2 carbon in the $\theta = 0.0°$ orientation. The h_2 hybrid is not pure $xz + yz$ but contains z^2: $h_2 = 0.55\ (xz + yz) + 0.1\ (z^2) + \ldots$ (eq 4). The h_2 hybrid is tilted by admixture

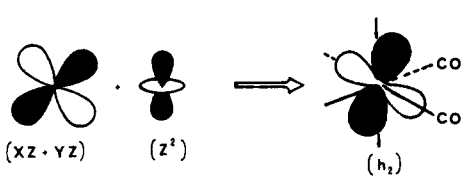

(4)

of z^2 so that in the $\theta = 0.0°$ orientation of the allyl, the *terminal carbons* (C_1 and C_3) dominate the group overlap, $\langle\pi|h_2\rangle$. Conversely, in the $\theta = 180°$ orientation, the *central carbon* (C_2) dominates the group overlap, $\langle\pi|h_2\rangle$.

Scheme I

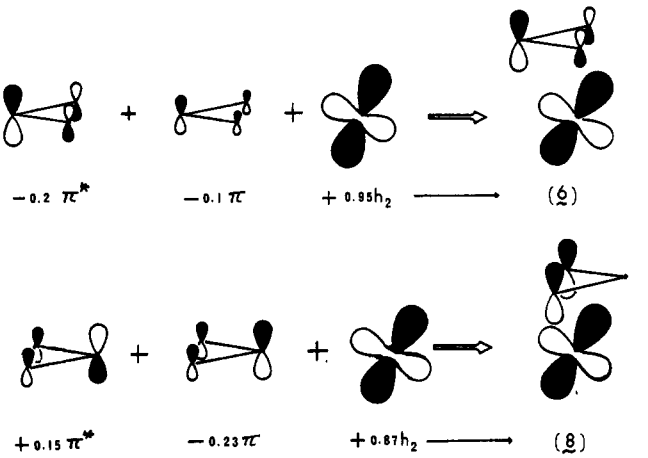

$\theta = 0.0°$: C_1 and C_3 in the π-FMO dominate its antibonding overlap with h_2. $\theta = 180°$: C_2 in the π-FMO dominates its antibonding overlap with h_2.

Now we can understand the different mixing of π and π^* in 6 and 8. The h_2 orbital interacts with π^* in a bonding fashion and with π in an antibonding fashion, but the relative phases of the π and π^* orbitals will be different in the two rotamers due to the different, dominant atomic overlaps. The diagrams in Scheme I illustrate this point. Mixing of π and π^* orbitals of complexed allyl groups through the metal orbitals has been discussed previously by Schilling et al.[11]

The different relative phases of the mixing of π and π^* via the metal hybrid h_2 causes a better bonding to the central carbon of the η^3-allyl group in the $\theta = 0.0°$ orientation. The different phases are a consequence of the mixing of z^2 and $(xz + yz)$ as shown in eq 3 and 4. The final question is, therefore, "why are the z^2 and $(xz + yz)$ mixed as shown?" There is no *direct* overlap between the σ-symmetry z^2 and the π-symmetry $(xz + yz)$ hybrid. Therefore, these orbitals cannot be mixed (or hybridized) in a first-order fashion.

It turns out that these orbitals are mixed via the agency of the π^* orbitals of the carbonyl groups. The σ bonding interactions mix 5s and $5p_z$ into z^2 in order to minimize the antibonding interactions between z^2 and the ligand σ orbitals; i.e., z^2 is hybridized to point out toward the vacant coordination site. The asymmetry of the $(s + p + z^2)$ hybrid with respect to xy plane now gives a nonzero overlap with the carbonyl π^* orbitals, which are mixed into the σ FMO in a bonding manner (10).

(10) (11)

The $(xz + yz)$ hybrid has the correct symmetry to back-bond to the carbonyl π^* orbitals as shown in 11. The net overlap between 10 and 11 is now nonzero *as a consequence of the commonage of the carbonyl π^* orbitals* in the fragment MO's. The orbitals 10 and 11 therefore interact in the well-known second-order formalism[10] with

(11) Schilling, B. E. R.; Hoffmann, R.; Faller, J. W. *J. Am. Chem. Soc.* **1979**, *101*, 592.

Chart I

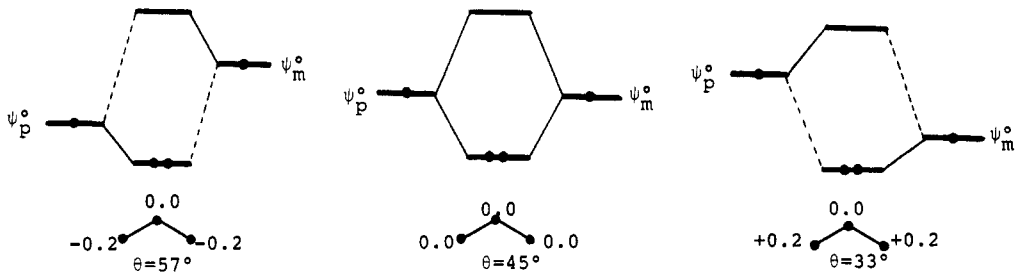

the lower one (**11**) being stabilized and the higher one (**10**) being destabilized (cf. eq 3 and 4).

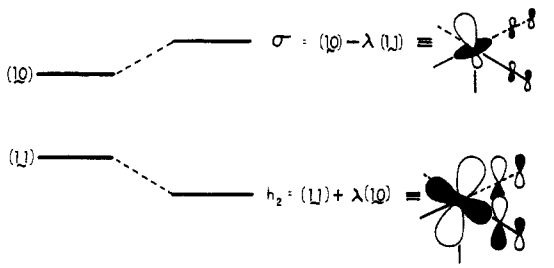

These results may be summarized as follows: The rotational preference of the allyl group in d^4 $X_3(CO)_2Mo(\eta^3\text{-}C_3H_5)$ complexes has its roots in the strong d–π^* back-bonding to the cis carbonyl ligands. The ($s + p_z + z^2$) orbital, **10**, of the $X_3(CO)_2Mo$ fragment is mixed into the ($xz + yz$) orbital, **11**, via the carbonyl π^* orbitals. This mixing causes a tilt in the ($xz + yz$) orbital to give h_2 (eq 4). The tilted hybrid, h_2, has a much better overlap with the allyl π orbital in the $\theta = 180$ orientation. Since the π orbital is lower in energy than h_2, the energy of the latter is pushed up by the π–h_2 interaction, and the better π–h_2 overlap in the $\theta = 180°$ orientation therefore causes a greater destabilization of h_2 relative to the $\theta = 0.0°$ orientation of the allyl group.

Regioselectivity of Nucleophilic Addition. It has been observed that a wide variety of nucleophiles are capable of addition to polyenes when the latter are coordinated to transition-metal species. Davies, Green, and Mingos[12] (DGM) have reviewed these reactions and have observed that three simple rules may be used to predict the regioselectivity of nucleophilic addition. These rules are as follows.[12]

Rule 1. Nucleophilic attack occurs preferentially at *even* coordinated polyenes which have no unpaired electrons in their HOMO.

Rule 2. Nucleophilic addition to *open* coordinated polyenes is preferred to addition to closed (i.e., cyclic) polyenes.

Rule 3. For *even open* polyenes nucleophilic attack at the terminal carbon atom is always preferred; for *odd open* polyenyls attack at the terminal carbon atom occurs only if ML_n^+ is a strong electron-withdrawing group.

With the exception of the last part of rule 3, these principles are straightforward and easy to apply to any given complex. However, application of rule 3 for *odd open* polyenyls (e.g., η^3-allyl) requires that an a priori judgement be made about the electron-withdrawing capability of a particular metal fragment. Rule 3 was rationalized by DGM using a perturbation approach which considered the effect of complexation on the charge distribution in the HOMO of the polyenyl fragment. The wave function is written as $\psi = \psi_p^0 \sin\theta + \psi_m^0 \cos\theta$, where ψ_p^0 and ψ_m^0 are the wave functions of the polyene *HOMO* and the metal fragment orbital, respectively. When $\theta = 0°$, the electrons are completely localized on the metal ($\psi \approx \psi_m^0$), the metal fragment is strongly electron withdrawing and the charge on the polyene is 1+.[13] When $\theta = 90°$, the metal is a very poor acceptor, the electrons are localized on the polyene ($\psi \approx \psi_p^0$), and the charge on the polyene is 1−. In the case of η^3-allyl complexes, the charge distribution in the HOMO (i.e., the nonbonding orbital, n) is shown in Chart I for three values of θ.[12]

Thus, when only the HOMO is considered, a strongly electron-withdrawing group imparts a partial positive charge on the terminal carbons and these are then the sites of nucleophilic attack. When the metal fragment is strongly electron releasing ($\theta > 45°$), then the terminal carbons are negative and the nucleophile then prefers attack at the central carbon.

The above analysis by DGM[12] assumes that the regioselectivity of nucleophilic attack is *charge controlled*. If this is the case, then it is somewhat surprising that, of all the allyl complexes examined to date, only the Cp_2M^+ (M = Mo, W) fragment is sufficiently "electron releasing" to direct nucleophilic attack to the central carbon (cf. eq 2). Furthermore, our calculations show that without exception the central carbon is positive with respect to the terminal carbons in η^3-allyl complexes. (A discussion of the factors that govern the charge distribution is given later.) Therefore we propose that the regioselectivity of nucleophilic attack on η^3-allyl complexes is *frontier orbital controlled* (FOC); i.e., the carbon undergoing nucleophilic attack must possess an empty low-energy orbital to accept the electrons on the incoming nucleophile. The more localized this acceptor orbital on the carbon in question, the better the incoming nucleophile is directed toward that carbon. Localization of the acceptor orbital is indicated by a large atomic orbital coefficient on the atom in question.

Since the HOMO of the allyl radical is the nonbonding orbital, n, and since this orbital lies close in energy to the d block orbitals, there is extensive mixing of the allyl n orbital and the metal d orbitals (corresponding to $\theta \approx 45°$ in the perturbation treatment). This mixing gives a filled bonding orbital in the complex, and an unfilled antibonding orbital of a″ symmetry. This a″ antibonding orbital is normally the LUMO of the metal–allyl complex and will normally be the acceptor orbital for an attacking nucleophile. Since this orbital has a *node* at the central carbon and large atomic coefficients on the terminal carbons, FOC normally will direct the nucleophile to the terminal carbons. With this general background, we now turn to specific examples.

(12) Davies, S. G.; Green, M. L. H.; Mingos, D. M. P. *Tetrahedron* **1978**, *34*, 3047; *Nouv. J. Chem.* **1977**, *1*, 445.

(13) This assumes the polyene is initially neutral. Thus, a neutral η^3-allyl complex is considered to result from the complexation of the allyl *radical* to a neutral metal fragment. In Figures 1–5 and 7, the electron occupancy of the fragments correspond to the allyl *anion* and a positively charged metal. The final electron distribution in the complex is independent of the convention, of course.

$X_3(CO)_2(\eta^3\text{-}C_3H_5)Mo^{II}$. The LUMO of $X_3(CO)_2Mo(\eta^3\text{-}C_3H_5)$ is the antibonding combination **5** of the nonbonding allyl orbital (n) and the $xz - yz$) hybrid (h_1) of the $X_3(CO)_2Mo$ fragment. This LUMO has a much lower energy than the other empty MO's and is the only acceptor orbital energetically available. Therefore, attack on the $X_3(CO)_2Mo(C_3H_5)$ complex by a nucleophile would be directed toward the end carbons (C_1 and C_3) of the allyl group.[11] Recently, Trost and Lautens have found that carbon nucleophiles do attack $L_2X(CO)_2Mo(C_3H_5)$ at the terminal carbons of the allyl group.[14] Furthermore, they observed a change in the regioselectivity as a function of the ligands on the metal. Complex **12** gave >95% selectivity as shown in eq 5, but complex **13** gave a 1:1 mixture of the two isomers as shown in eq 6.

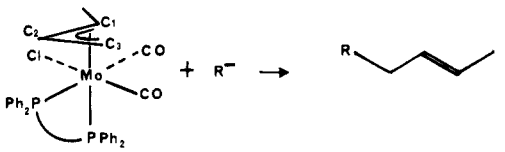

(5)

(12)

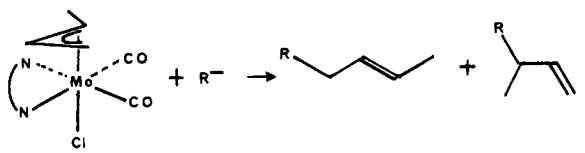

(6)

(13)

The difference in regioselectivity exhibited by **12** and **13** may be rationalized by our calculations. The electronic asymmetry of the P and Cl ligands in **12** is reflected in the C_1 and C_3 $2p_z$ coefficients in the LUMO, viz., −0.28 and 0.32, respectively.[11] Thus, if steric repulsion between the methyl substituent on the η^3-allyl group and the bulky diphos ligand favors the orientation shown in **12**, then an incoming nucleophile would be directed toward C_3, i.e., to the position with the larger atomic coefficient which gives the linear olefin.

Other orientations, e.g., **14** or **15**, show even larger differences in the LUMO coefficients between C_1 and C_3, e.g., −0.19 and 0.30 for **14**.[15] Therefore, if these conformations

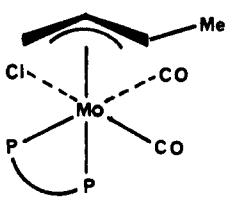

(14)

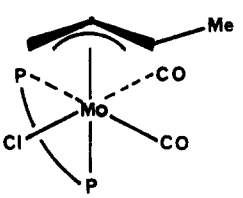

(15)

are favored by steric interactions, the frontier orbital controlled regioselectivity could be quite pronounced as observed experimentally. Conversely, the coefficients of C_1 and C_3 in **13** have essentially equal magnitudes, and no regioselectivity is expected, a result which is also in accord with experiment.

It is unlikely that such a simple picture as given above will be generally useful. Although attack at a terminal carbon is clearly indicated, the particular terminal carbon that will undergo attack is likely to be influenced by several factors, e.g., steric bulk of the nucleophile and the substituents on the allyl group, the charge distribution, and

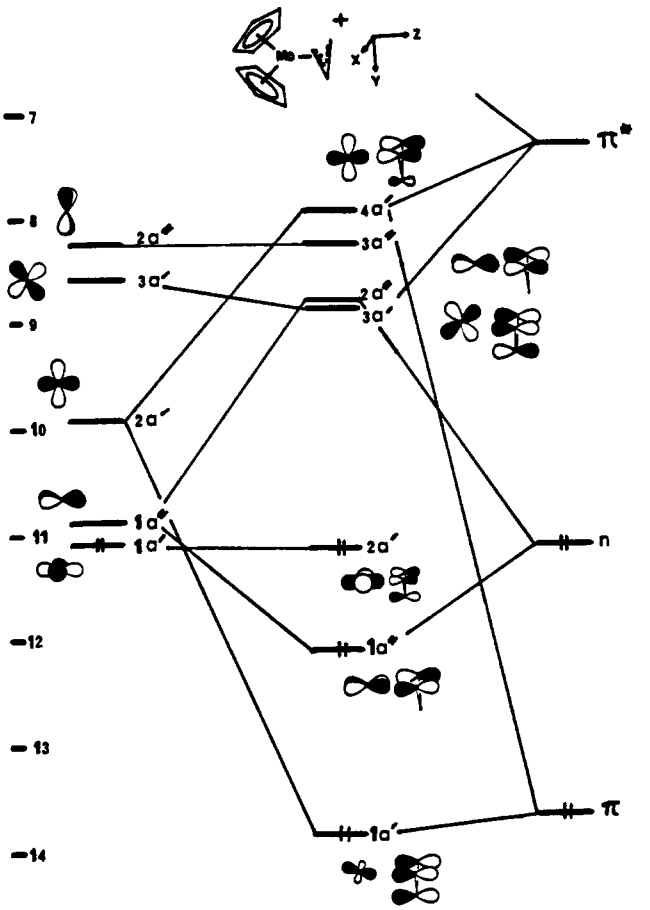

Figure 3. EHMO energy level diagram for $Cp_2Mo(\eta^3\text{-allyl})^+$.

the hardness or softness of the nucleophile.

$Cp_2Mo(\eta^3\text{-}C_3H_2)^+$. As stated previously, $Cp_2M(\eta^3\text{-}C_3H_5)^+$ (M = Mo, W) are the only known examples in which nucleophilic attack occurs at the central carbon of the allyl group, and a significant difference between the ordering of the LUMO's of $X_3(CO)_2Mo(\eta^3\text{-}C_3H_5)^+$ (Figure 1) and $Cp_2Mo(\eta^3\text{-}C_3H_5)^+$ (Figure 3) is immediately evident:[16] the Cp_2Mo^{2+} fragment possesses a high-lying symmetric orbital (the 3a′—mostly yz) of the correct symmetry to interact with the high-energy π^* orbital of the allyl group. This interaction gives a symmetric orbital (3a′) just below or nearly degenerate with[17] the 2a″ MO composed of the antibonding combination of the allyl nonbonding (n) orbital with the 1a″ (xz) orbital of the Cp_2M fragment. The 2a″ MO would direct the incoming nucleophile to the terminal carbons as in the case of the $X_3(CO)_2Mo(\eta^3\text{-}C_3H_5)$ complexes. The 3a′ orbital, on the other hand, features an acceptor site on the central carbon. The interaction of the donor orbital of the incoming nucleophile with the central carbon in the 3a′ orbital smoothly leads to an allowed, disrotatory ring closure to the metallocyclobutane (eq 7).

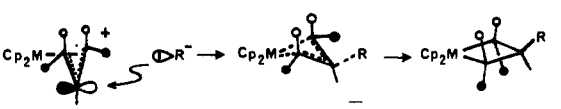

(7)

Why is it that the $2p_z$ orbital on the central carbon acts as the acceptor site for an incoming nucleophile, rather

(14) Trost, B. M.; Lautens, M. *J. Am. Chem. Soc.* **1982**, *104*, 5543.
(15) The larger asymmetry of the C $2p_z$ coefficients in the LUMO corresponding to the $\theta = 90°$ orientation is caused by the allyl n orbital interacting with the tilted FMO h_2 (see Figure 1).
(16) $Cp_2M(\eta^3\text{-}C_3H_5)$ complexes have been treated previously, but the levels of interest here were not discussed: Lauher, J. W.; Hoffmann, R. *J. Am. Chem. Soc.* **1978**, *98*, 1729.
(17) The exact placement of 3a′ relative to 2a″ depend slightly on the placement of the allyl moiety with respect to the Cp_2Mo fragment. The slight variation observed does not affect the arguments developed here.

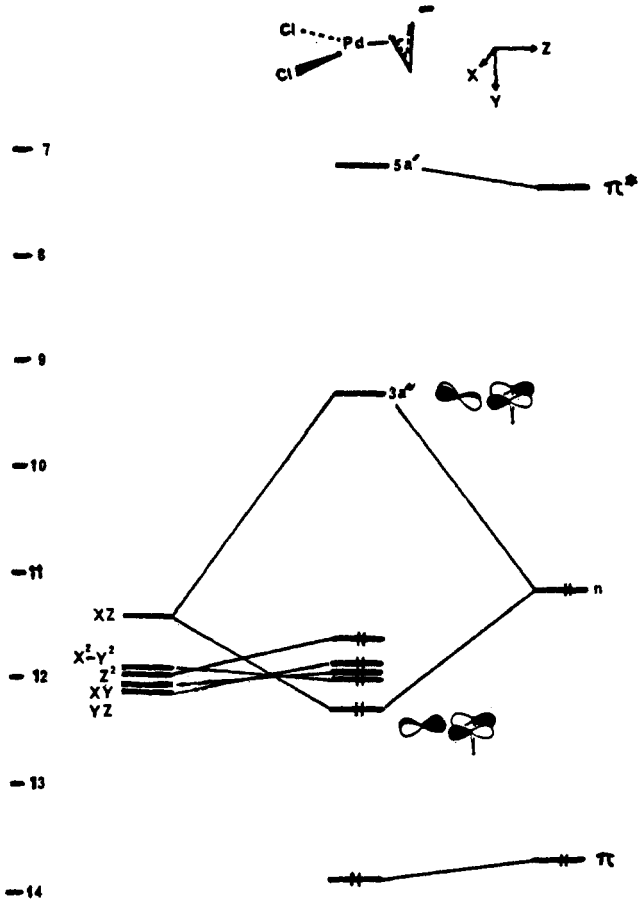

Figure 4. EHMO energy level diagram for $Cl_2Pd(\eta^3\text{-allyl})^-$.

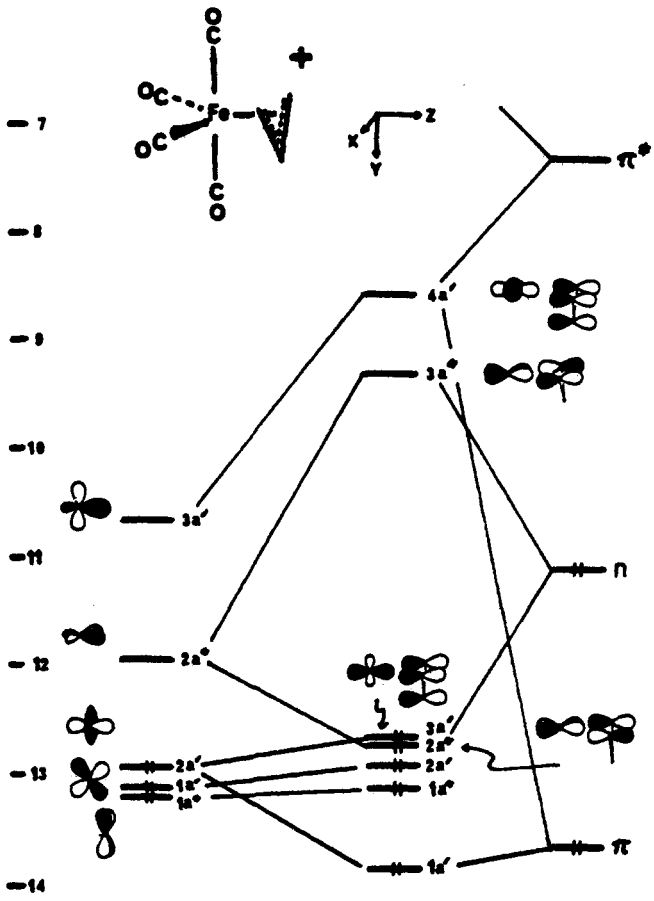

Figure 5. EHMO energy level diagram for $(CO)_4Fe(\eta^3\text{-allyl})^+$.

than the equally available $2p_z$ orbitals on the terminal carbons? In the 3a′ orbital, the C $2p_z$ coefficients for the central and terminal carbons are 0.25 and −0.17, respectively. Furthermore, the central carbon is positive with respect to the terminal carbons, so that charge and FOC work in concert to direct the nucleophile to the central carbon.

$L_2Pd(\eta^3\text{-}C_3H_5)$. $L_2Pd(\eta^3\text{-allyl})$ complexes are known to react with nucleophiles to give olefins and this reaction has been developed as a carbon–carbon bond-forming synthesis in organic chemistry.[1b,18] The results of our calculation on the model compound $Cl_2Pd(\eta^3\text{-}C_3H_5)^-$ are shown in Figure 4. The LUMO is the antisymmetric 3a″ orbital that directs nucleophilic attack to the terminal carbons. The symmetric orbital 5a′ is energetically unaccessible so that we expect only olefin formation as observed experimentally (eq 8).[18,19]

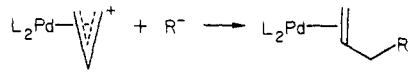

(8)

$(CO)_4Fe(\eta^3\text{-}C_3H_5)^+$. According to the results of Elian and Hoffmann,[20] a C_{2v} $M(CO)_4$ fragment might have a low-energy a′ orbital which could interact with the allyl π^* MO, producing a low-energy symmetric acceptor orbital in $(CO)_4M(\eta^3\text{-}C_3H_5)^+$ which would direct attack to the central carbon. Our results for $(CO)_4Fe(\eta^3\text{-}C_3H_5)^+$ are shown in Figure 5. Although the $(CO)_4Fe$ fragment indeed has an a′ orbital close in energy to π^*, this 3a′ orbital is of σ symmetry with respect to the allyl group. Consequently, the strongest interaction of the 3a′ FMO of the $Fe(CO)_4^{2+}$ fragment is with the allyl π orbital. This interaction leads to the 4a′ MO which lies about 0.7 eV above the 3a″ MO of the $Fe(CO)_4(\eta^3\text{-}C_3H_5)^+$ molecule (Figure 5). The C_2 $2p_z$ coefficient in the 4a′ MO is relatively small, 0.13. The high energy of the 4a′ orbital, combined with the small coefficient at C_2, leads to the prediction that nucleophilic attack on $Fe(CO)_4(\eta^3\text{-}C_3H_5)^+$ would be directed to the terminal carbons of the allyl group. Experimentally, compounds of the type $Fe(CO)_4(\eta^3\text{-allyl})^+$ react with nucleophiles to give olefins (eq 9).[21]

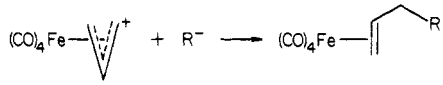

(9)

Generalizations. Suppose one wished to search for other η^3-allyl complexes that would give matallacyclobutanes upon reaction with nucleophiles, what are the electronic requirements for such a transformation? Ideally, the *yz* oribtal of the metal fragment should lie somewhat below the π^* orbital of the allyl fragment. (The problem with the $Fe(CO)_4^{2+}$ fragment is that the *yz* orbital lies *too* low! It is not destablized by σ interactions and is stabilized by back-bonding to CO π^* orbitals.) In order to destabilize the *yz* orbital, ligands should be placed in the *yz* plane as shown in **16**. If L and L′ differ significantly in their

(18) Trost, B. M.; Weber, L.; Strege, P. E.; Fullerton, T. J.; Dietsche, T. J. *J. Am. Chem. Soc.* **1978**, *100*, 3416.

(19) Olefins may be formed by nucleophilic addition to $L_2M(\eta^3\text{-}C_3H_5)^+$ (M = Pd, Pt) either by direct addition to the allyl fragment or by addition of the nucleophile to the metal followed by reductive elimination. The work in ref 18 indicates direct attack of soft carbanions on the coordinated allyl moiety.

(20) Elian, M.; Hoffmann, R. *Inorg. Chem.* **1975**, *14*, 1058.

(21) Deeming, A. J. *Compr. Organomet. Chem.* **1982**, *4*, 423.

Table I. Selected Calculated Values for CpML $(\eta^3\text{-}C_3H_5)^+$

M	L	ϕ^a	ΔE^b	% π^c	% π^{*c}	% 3a′ ^{c}	$C_2{}^d$	$S_\pi{}^e$	$S_{\pi^*}{}^e$	type^f
Co	PH_3	90	0.53	13	2	86	0.08	0.204	0.037	3
Co	PH_3	112	0.17	11	0.0	86	0.16	0.204	0.005	1
Co	CO	90	0.57	12	2	85	0.08	0.215	0.037	3
Rh	PH_3	90	0.70	8	16	66	0.18	0.271	0.058	3
Rh	PH_3	112	0.31	7	8	71	0.07	0.259	0.026	3
Rh	CO	90	0.47	3	14	30	0.24	0.286	0.057	2-3

[a] Dihedral angle between the allyl plane and the xz plane. [b] Energy separation (eV) between the 4a′ and 3a″ molecular orbitals. [c] % contribution of the allyl π and π^* and the CpML fragment 3a′ orbitals to the 4a′ molecular orbital. [d] Value of the C_2 ($2p_z$) atomic orbital coefficient in the 4a′ MO. [e] Group overlap integrals $\langle 3a' | \pi \rangle$ and $\langle 3a' | \pi^* \rangle$. [f] Classification according to Figure 6 and discussion in text.

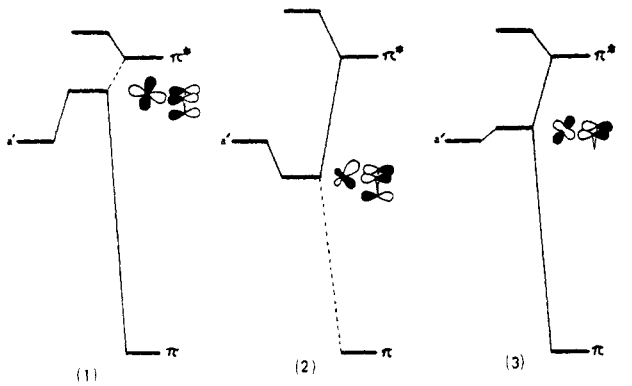

Figure 6. Types of interaction between metal a′ orbital and the allyl π and π^* orbitals. See text for description.

σ-bonding properties, the symmetric σ-type orbitals, $x^2 - y^2$ and z^2, will mix into the π-type yz orbital to give the tilted hybrids, e.g., 17 and 18. As the admixture of σ-type orbitals, e.g., z^2 into the yz increases, the overlap with the allyl π^* orbital decreases while the overlap with the allyl π orbital increases. These hybridization effects lead to three types of interaction schemes (Figure 6).

Type 1: much σ-type character in the metal a′ orbital and strong interaction with the allyl π orbital. Result: destabilization of the a′ orbital, moderate to large coefficient for C_2 $2p_z$ orbital in final MO.

Type 2: much π-type (yz) character in the metal a′ orbital and strong interaction with the allyl π^* orbital. Result: the ideal situation for metallacycle formation—the a′ orbital is stabilized and may become the LUMO and the C_2 $2p_z$ coefficient is large.

Type 3: intermediate between cases 1 and 2, i.e., moderate interaction of the metal a′ orbital with *both* the allyl π and π^* orbitals. Result: not much perturbation of the energy of the metal a′ orbital *but* the C_2 $2p_z$ coefficient will be very small as a result of the out-of-phase mixing of the π and π^* orbitals (cf. Scheme I).

According to this classification, $(CO)_4Fe(allyl)^+$ and $X_3(CO)_2Mo(allyl)^+$ display type 1 behavior, $Cp_2Mo(allyl)^+$ displays type 2, and $L_2Pd(allyl)^+$ complexes have no high energy a′ orbital.

From the analysis presented above, the family of complexes $CpLM(\eta^3\text{-}C_3H_5)^+$ (L = CO, PR_3; M = Co, Rh, Ir) (19) might be suitable as substrates for metallacycle for-

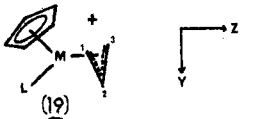

(19)

mation. The results of our calculations for a sample of these molecules are shown in Figure 7 and Table I. Since no structural data are available of these complexes, a very limited mapping of the potential surface was undertaken. The orientation of the allyl group shown in 19 is considerably more stable than the alternative rotamers, and slight movement of the allyl group up or down along the y axis had little effect on the results. Tilting the plane of the allyl group give slight variations in energy but had a strong effect on the value of the $2p_z$ coefficient at C_2. Table I shows the results for the limiting tilts of the allyl: $\phi = 90°$ places the allyl group parallel to the xy plane and $\phi = 112°$ swings the central carbon away from the metal.

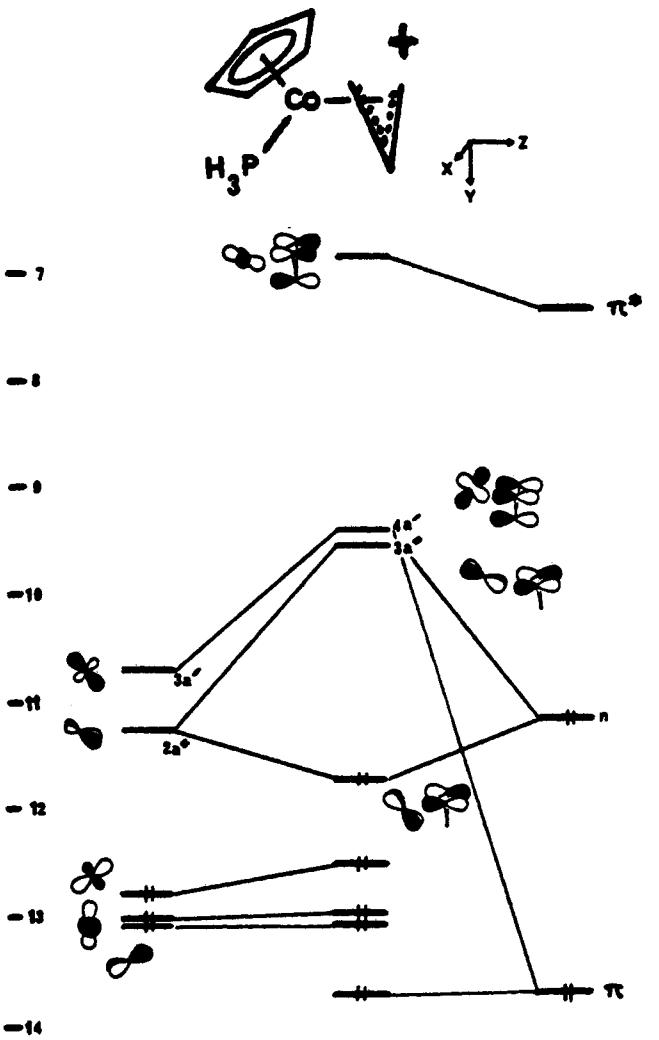

Figure 7. Representative EHMO energy level diagram for $CpLM(\eta^3\text{-allyl})^+$ (M = Co, Rh; L = CO, PH_3) complexes.

All the energy level diagrams computed for 19 show the same general features: the LUMO is the 3a″ orbital from the allyl nonbonding orbital and the symmetric 4a′ orbital lies at slightly higher energy. Table I lists the computed separation, ΔE, between the 3a″ and 4a′ orbitals, the percent contribution of the allyl π and π^* orbitals for the 4a′ MO, the value of the $2p_z$ coefficient on C_2, the values of the group overlap integrals of the allyl π or π^* orbitals

Table II. Charge Redistribution in the Complexed Allyl Radicals $L_nM(allyl)$

ML_n	$\rho_\pi(a')$ C_1	$\rho_\pi(a')$ C_2	$\rho_\pi(a'')$ C_1	$\Delta e(a')^a$	$\Delta e(a'')^a$	q_π C_1	q_π C_2	q_T C_1	q_T C_2
$Cp(CO)Co^+$	0.53	0.93	0.48	−0.01	−0.03	−0.01	+0.07	−0.09	+0.09
$Cp(CO)Rh^+$	0.49	0.83	0.61	−0.19	+0.22	−0.10	+0.17	−0.23	+0.04
Cp_2Mo^+	0.58	1.07	0.62	+0.23	+0.24	−0.20	−0.07	−0.28	+0.06
$(CO)_4Fe^+$	0.52	0.94	0.49	−0.03	−0.03	−0.01	+0.06	−0.07	+0.15
Cl_2Pd	0.54	0.89	0.49	−0.02	−0.02	−0.03	+0.11	−0.15	+0.03
$(HCN)_3(CO)_2Mo^+$	0.42	0.78	0.30	−0.38	−0.39	+0.17	+0.22	−0.08	+0.02
$Cl_3(CO)_2Mo^-$	0.48	0.90	0.44	−0.14	−0.01	+0.08	+0.10	−0.06	+0.03

[a] Number of electrons transferred to or from C_3H_5. A negative value indicates electron donation from the neutral C_3H_5 radical to ML_n and vice versa for a positive value.

and the 3a′ FMO, and the classification according to the types 1–3 discussed above.

The complexes **19** seem to present a dilemma. Adjusting the ligand, L, or the angle, ϕ, to minimize ΔE tends to mix the π and π^* FMO's to give a small coefficient at C_2. Thus, at $\phi = 90°$ $Cp(H_3P)Rh(\eta^3\text{-}C_3H_5)^+$ has a reasonable value of the C_2 $2p_z$ coefficient (0.18) which could lead to attack at C_2, but the 4a′ level lies 0.7 eV above the 3a″ level. The high energy of the 4a′ level would decrease its ability to act as an acceptor orbital. At $\phi = 112°$, ΔE decreases to 0.31 eV, but the C_2 $2p_z$ coefficient drops to 0.07 as a result of more extensive mixing of π and π^*. The best case for central carbon attack seems to be $Cp(H_3P)Co(\eta^3\text{-}C_3H_5)^+$, at $\phi = 112°$. In this case, ΔE is only 0.17 eV and the C_2 $2p_z$ coefficient has a value of 0.16. In summary, it seems that $CpLM(\eta^3\text{-}C_3H_5)^+$ would probably suffer attack at a terminal carbon, but there is a chance that charge control might dominate in certain instances to give attack at the central carbon.

As can be seen from Figure 3, a complex of the type $Cp_2M(\eta^3\text{-}C_3H_5)^+$ (M = Ti, Zr, Hf), which have two electrons less than the corresponding Mo or W complex, would have the 2a′ MO unfilled. This MO features a large coefficient on the C_2 $2p_z$ carbon, so that these group 4, $Cp_2M(allyl)^+$, complexes might also form metallacyclobutanes upon nucleophilic attack. Work is currently in progress to determine the regioselectivity of nucleophilic attack on $CpLM(allyl)^+$ (M = Co, Rh) and $Cp_2M(allyl)^+$ (M = Ti, Zr) complexes.

Conclusions

The rotational preference of the η^3-allyl group in complexes of the type $X_3(CO)_2Mo(\eta^3\text{-allyl})$ has been shown to be the result of a second-order mixing of σ- and π-type orbitals on the metal through the carbonyl π^*-orbitals. This mixing produces a hybrid that bonds best to the allyl when the allyl group has its open face toward the carbonyls. At least 16 structures of $X_3(CO)_2Mo(allyl)$ show this feature.

The regioselectivity of nucleophilic attack on the coordinated allyl moiety has been shown to be dominated by frontier orbital control. In all cases in which attack at the terminal carbon of the allyl moiety is known to occur, the LUMO (acceptor orbital) is an antisymmetric orbital with a node on the central carbon and large coefficients for the terminal carbon $2p_z$ atomic orbitals. In the one case in which attack occurs on the central carbon, the LUMO is a symmetric orbital with a large coefficient on the positively charged central carbon. Although the electronic requirements on the metal fragment are so stringent that relatively few allyl complexes are expected to form metallacycles upon nucleophilic attack, the analysis presented here should aid considerably in the design of synthetic strategies toward that goal.

Postscript: Charge Redistribution in the Complexed Allyl Group. Even though a detailed understanding of the origin of the charge distribution in a complexed allyl group is not vital to the arguments on regioselectivity presented above, it is nevertheless of interest to examine the flow of charge which occurs when a free allyl radical is bonded to a transition-metal fragment. In a free allyl radical, the π-electron densities (ρ_π) on the terminal (C_1) and central (C_2) carbons are (0.5, 1.0) and (0.5, 0.0) (C_1, C_2) in the π and n orbitals, respectively. Table II shows how these densities are altered when the radical is complexed. The entry $\rho_\pi(a')$ is the sum of the electron density in the allyl π and π^* orbitals (the latter is populated by "back donation" from the metal); $\rho_\pi(a'')$ is the density in the allyl HOMO (nonbonding orbital). Δe is the net gain or loss of electrons, q_π the charge produced by the electron density in the π system (a′ + a″), and q_T the total atomic charge.

In contrast to the assumption made by DGM, it is seen that the charge flow in the a′ orbitals is not insignificant and results in a net loss of electrons (primarily from C_2) for all complexes except $Cp_2Mo(allyl)^+$. In this complex, the 1a′ FMO on the metal donates electrons into the allyl π^* orbital (acceptor) to give the 2a′ MO of the complex (see Figure 3).

The charge transfer in the a″ orbitals should be comparable to those obtained in the DGM perturbation approach. The Cp_2Mo^+ and $Cp(CO)Rh^+$ fragments are "electron rich" in the DGM scheme since their d orbitals lie at relatively high energies. Indeed, these fragments *donate* about 0.2 e into the allyl HOMO corresponding to a θ value of ca. 50° in the DGM scheme. In the remaining complexes, the allyl HOMO suffers a slight to moderate

Table III. Atomic Parameters Used in the EHMO Calculations

orbital		H_{ii}, eV	ζ	orbital		H_{ii}, eV	ζ
H	1s	−13.60	1.300	O	2s	−32.30	2.275
C	2s	−21.40	1.625		2p	−14.80	2.275
	2p	−11.40	1.625	Cl	3s	−30.00	2.033
N	2s	−26.00	1.950		3p	−15.00	2.033
	2p	−13.40	1.950				

orbital		H_{ii}, eV	ζ_1	ζ_2	C_1[a]	C_2[a]
Fe	4s	−9.10	1.900			
	4p	−5.32	1.900			
	3d	−12.60	5.35	2.000	0.5505	0.6260
Co	4s	−9.21	2.000			
	4p	−5.29	2.000			
	3d	−13.18	5.550	2.100	0.5679	0.6059
Mo	5s	−8.77	1.960			
	5p	−5.60	1.900			
	4d	−11.06	4.540	1.900	0.5899	0.5899
Rh	5s	−8.09	2.135			
	5p	−4.57	2.100			
	4d	−12.50	4.290	1.970	0.5807	0.5685
Pd	5s	−7.32	2.190			
	5p	−3.45	2.152			
	4d	−12.02	5.983	2.613	0.5264	0.6373

[a] Coefficients in the double ζ expansion.

loss of electrons ($\theta \approx 40$–$45°$).

The total electron density at a particular carbon (C_μ) is the sum of the densities in the a′ and a″ orbitals at that carbon, $\rho_T^\mu = \rho_\pi^\mu(a') + \rho_\pi^\mu(a'')$, and the π-charge is then $q_\pi^\mu = 1.0 - \rho_T^\mu$. The values in Table II show that in all cases, q_π for the central carbon (C_2) is more positive than q_π for the terminal carbon (C_1). Hence, charge control would always direct an incoming nucleophile to the central carbon contrary to what is experimentally observed.

The total charge (q_T) on the allyl fragment includes charges incurred in the C–H σ bonds and in interactions of the allyl σ framework with the metal fragment (although these latter interactions are not large, there are many of them). Consequently the total charge differs from q_π, but the general trend is the same; namely, C_2 is always more positive than C_1.

Acknowledgment. This research was supported by the National Science Foundation (Grant No. CHE82-06153) and the donors of the Petroleum Research Fund, administered by the American Chemical Society. We also thank the Computing Center of the University of Michigan for computing time.

Appendix

An idealized geometry was used in the EHMO calculations. For the $X_3(CO)_2Mo$ fragments, the ligands were placed on the x, y, and z axes at appropriate distances (Mo–Cl = 2.50 Å; Mo–N = 2.10 Å, Mo–C = 2.00 Å, C–O = 1.15 Å; C–N = 1.16 Å; C–H = 1.0 Å). The allyl group lay in a plane parallel to the xy plane and 2.0 Å above it. The Mo–$C_{1,3}$ distance was 2.33 Å; M–C_2 was 2.14 Å, and the C–C–C angle was 116°. For the Cp_2Mo complex, the Mo–Cp centroid distance was 2.0 Å, and the Cp–Mo–Cp angle was 140°. The plane of the allyl group was 2.0 Å from the Mo (Mo–$C_{1,3}$ = 2.33 Å; Mo–C_2 = 2.14 Å). In the CpLM(allyl) complexes, the Cp–M–L angle was 120° and the Cp–Rh and Cp–Co distances were 1.90 and 1.70 Å, respectively. The allyl group was in planes 1.90 and 1.70 Å from the metal (Rh and Co, respectively). The atomic parameters used in the EHMO calculations are collected in Table III.[9] No attempt was made to adjust these parameters for the different overall charges on the complexes since it has been shown by charge iteration calculations that overall molecular charge has little effect on the EHMO parameters.[22]

Registry No. **2** (M = Mo, X = L = HCN), 89676-73-3; **2** (M = Mo, X = L = Cl), 89676-74-4; **12**, 62742-80-7; **13**, 86022-48-2; $Cp_2Mo(\eta^3\text{-}C_3H_5)^+$, 53449-94-8; $Cl_2Pd(\eta^3\text{-}C_3H_5)^-$, 35428-96-7; $(CO)_4Fe(\eta^3\text{-}C_3H_5)^+$, 49865-93-2; $CpCo(PH_3)(\eta^3\text{-}C_3H_5)^+$, 89676-75-5; $CpCo(CO)(\eta^3\text{-}C_3H_5)^+$, 71744-59-7; $CpRh(PH_3)(\eta^3\text{-}C_3H_5)^+$, 89676-76-6; $CpRh(CO)(\eta^3\text{-}C_3H_5)^+$, 89676-77-7.

(22) Hoffman, D. M.; Hoffmann, R. *Inorg. Chem.* **1981**, *20*, 3543. Somerville, R. H.; Hoffmann, R. *J. Am. Chem. Soc.* **1976**, *98*, 7240.

Molecular Orbital Studies of Organometallic Hydride Complexes. 2. The Correlation of Hydrogen Atom Reactivity with Valence Orbital Energetics

Bruce E. Bursten* and Michael G. Gatter

Department of Chemistry, The Ohio State University, Columbus, Ohio 43210

Received November 15, 1983

The relative acidic or hydridic strengths of several isostructural hydride complexes L_nM–H have been correlated with the valence orbital energetics of the deprotonated hydrides L_nM^-. The acidities of the carbonyl–phosphine proton donor series $HCo(CO)_{4-n}L_n$ (n = 0–3; L = PPh_3 or $P(OPh)_3$), $HMn(CO)_{5-n}L_n$, and $HV(CO)_{6-n}L_n$ (n = 0, 1; L = PPh_3) can be ranked within each series by the magnitude of the HOMO/LUMO separations found for their conjugate bases. Larger HOMO/LUMO gaps are calculated for the anions of the stronger acids. The relative hydridic strengths of Cp_2ML_nH (Cp ≡ η^5-C_5H_5; M = Zr, Nb, Mo; L = H, CO) hydride donors can be determined by both the magnitude of the HOMO/LUMO separations and the separations between the HOMO and the second highest occupied molecular orbital in the deprotonated species.

Introduction

Two different ionic dissociative routes are available to organometallic hydride complexes in polar solvents.[1]

$$L_nM\text{–}H \rightarrow L_nM^- + H^+ \quad \text{proton donor}$$

$$L_nM\text{–}H \rightarrow L_nM^+ + H^- \quad \text{hydride donor}$$

Although several research groups have recently reported systematic studies of the thermodynamic and kinetic reactivities of organometallic hydride systems,[2-4] very little is presently known about the electronic influences responsible for the proton or hydride dissociation from metal hydride complexes. We have recently reported[5] that the reactivity of the hydride ligand in L_nM–H hydride complexes is closely related to the orbital energies of the conjugate base L_nM^- as calculated by the Fenske–Hall molecular orbital method.[6] Indeed, we have found that the hydridic character of $CpM(NO)_2H$ (Cp ≡ η^5-C_5H_5; M = Mo, W) complexes vis-à-vis the acidic nature of the

(1) Schunn, R. A. In "The Hydrogen Series"; Muetterties, E. L., Ed.; Marcel Dekker: New York, 1971; Vol. 1, pp 203–269.
(2) Labinger, J. A.; Komadina, K. H. *J. Organomet. Chem.* **1978**, *155*, C25–C28.
(3) Jordan, R. F.; Norton, J. R. *J. Am. Chem. Soc.* **1982**, *104*, 1255–1263.
(4) Richmond, T. G.; Basolo, F.; Shriver, D. F. *Organometallics* **1982**, *1*, 1624–1628.
(5) Part 1: Bursten, B. E.; Gatter, M. G. *J. Am. Chem. Soc.* **1984**, *106*, 2554–2558.
(6) Hall, M. B.; Fenske, R. F. *Inorg. Chem.* **1972**, *11*, 768–775.

0276-7333/84/2303-0895$01.50/0